Achieving High-Performance OER Catalysis with Dual-Site Modulated Fe-Based Perovskites

Yixin Bi[a1], Yuhao Wang[a1], Yufei Song[d], Qing Chen[a*], Francesco Ciucci[a, b, c*]

a. Department of Mechanical and Aerospace Engineering, The Hong Kong University of Science and Technology, Clear Water Bay, Kowloon, Hong Kong S.A.R., China

b. University of Bayreuth, Chair of Electrode Design for Electrochemical Storage, Weiherstraße 26, 95448 Bayreuth, Bayreuth, Germany

c. University of Bayreuth, Bavarian Center for Battery Technology (BayBatt), Universitätsstraße 30, 95447 Bayreuth, Germany

d. State Key Laboratory of Materials-Oriented Chemical Engineering, College of Chemical Engineering, Nanjing Tech University, Nanjing, 210009, China

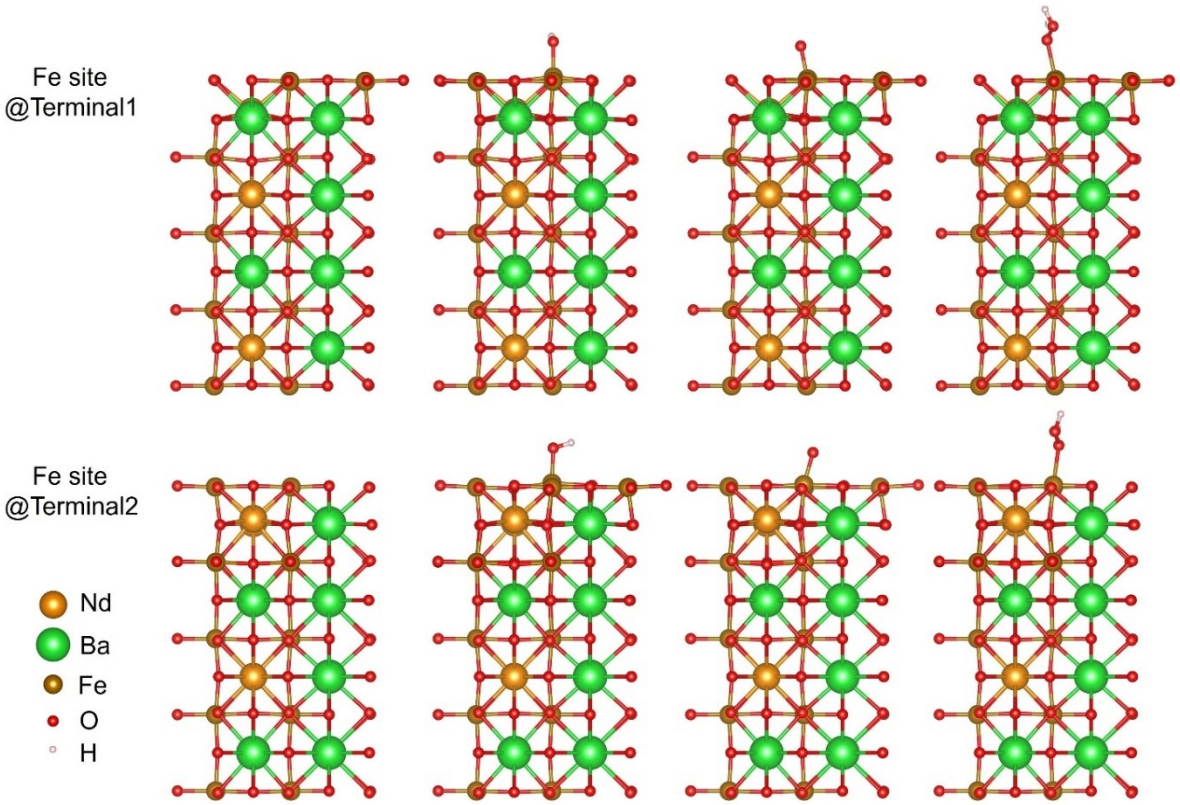

Figure S1 Schematic diagram illustrating the surface adsorption model for each step of OER on NBF.

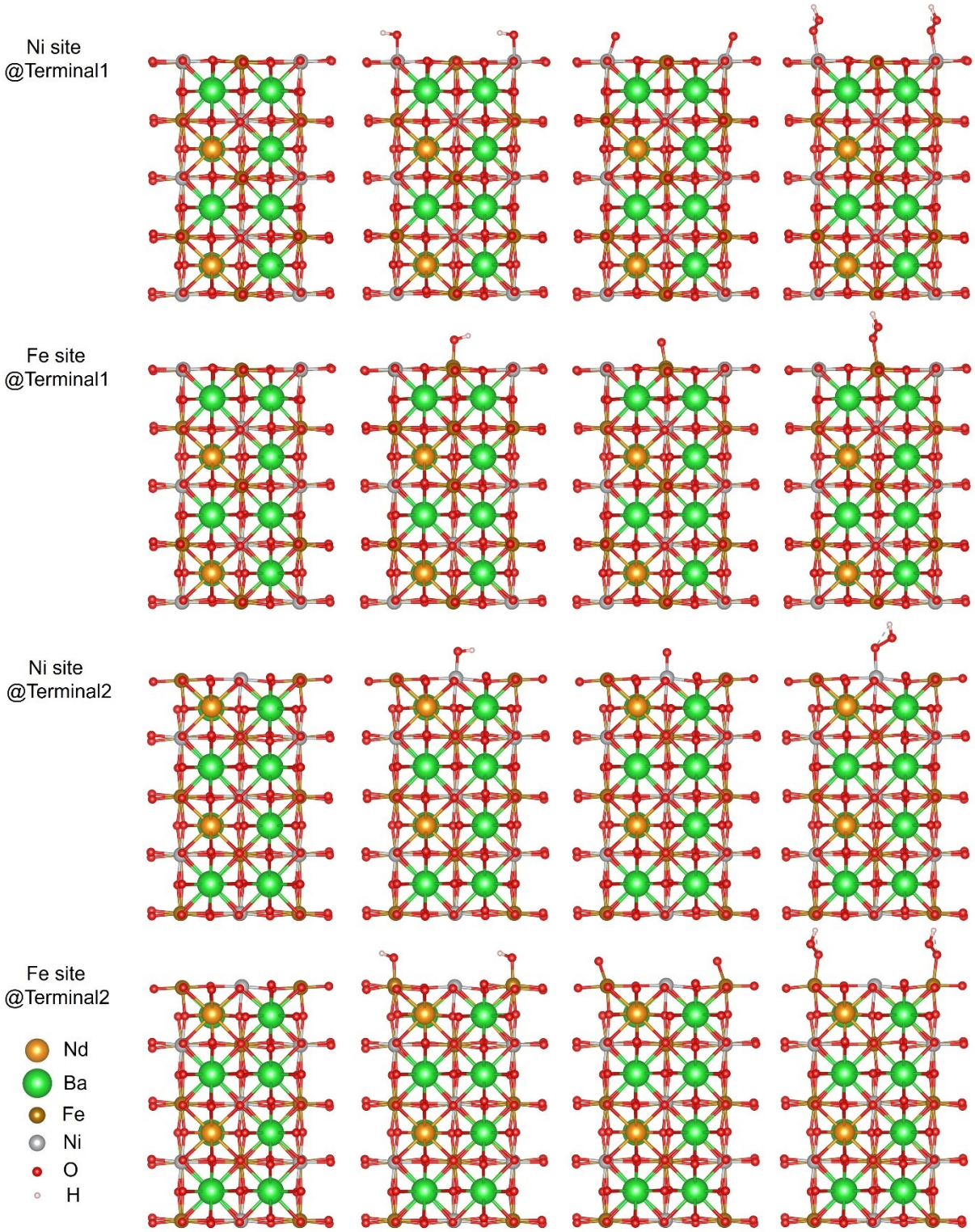

Figure S2 Schematic diagram illustrating the surface adsorption model for each step of OER on NBFN.

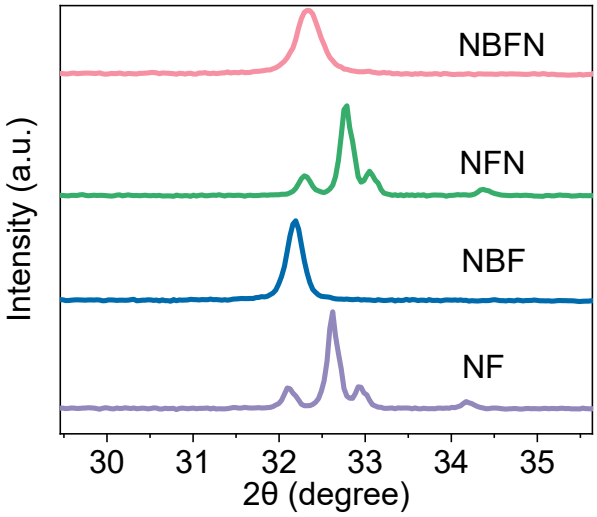

Figure S3 Magnified XRD pattern.

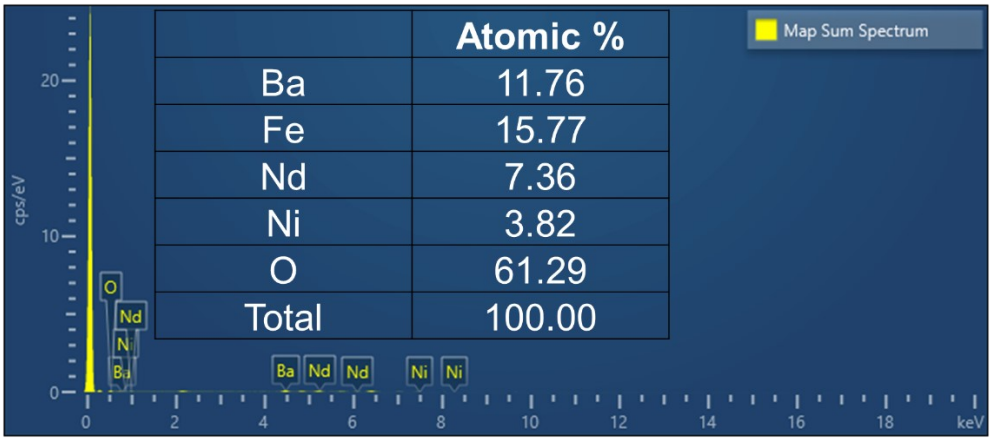

	Atomic %
Ba	11.76
Fe	15.77
Nd	7.36
Ni	3.82
O	61.29
Total	100.00

Figure S4 SEM-EDS results showing elements composition of NBFN.

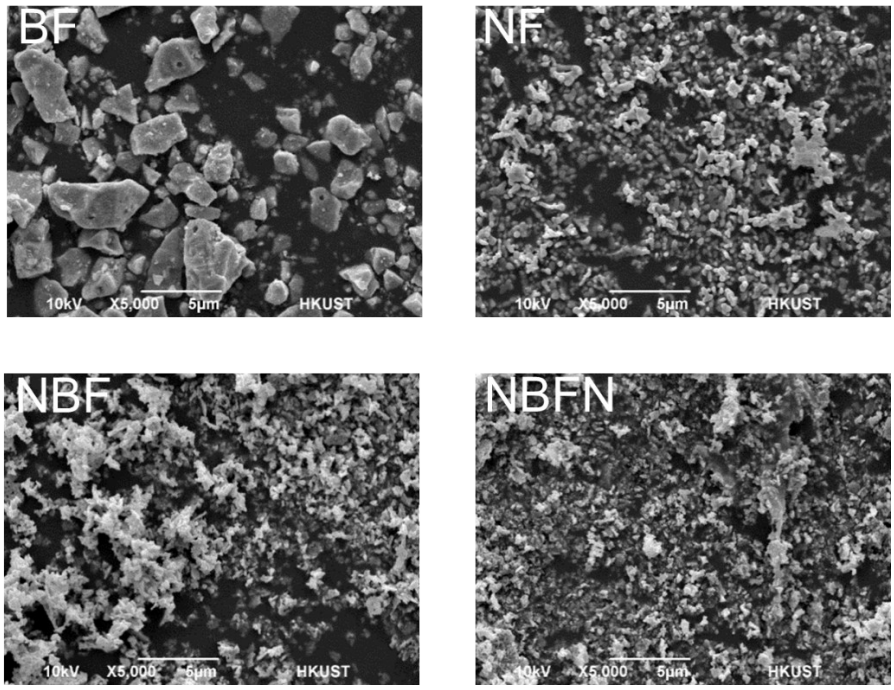

Figure S5 Morphology study of BF, NF, NBF and NBFN.

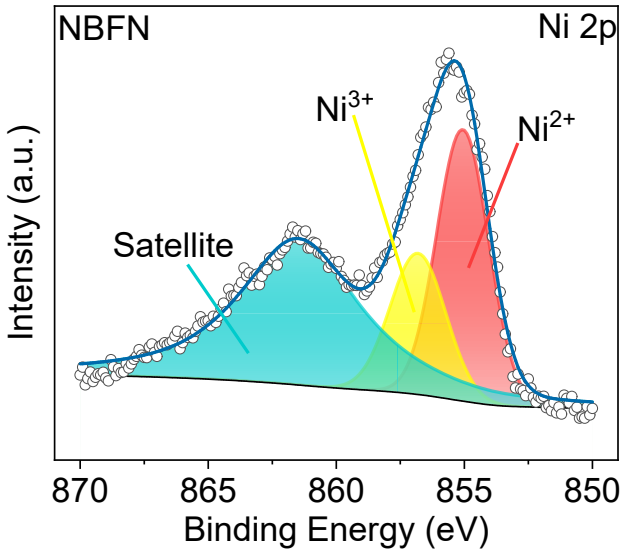

Figure S6 Ni 2p XPS spectra of NBFN.

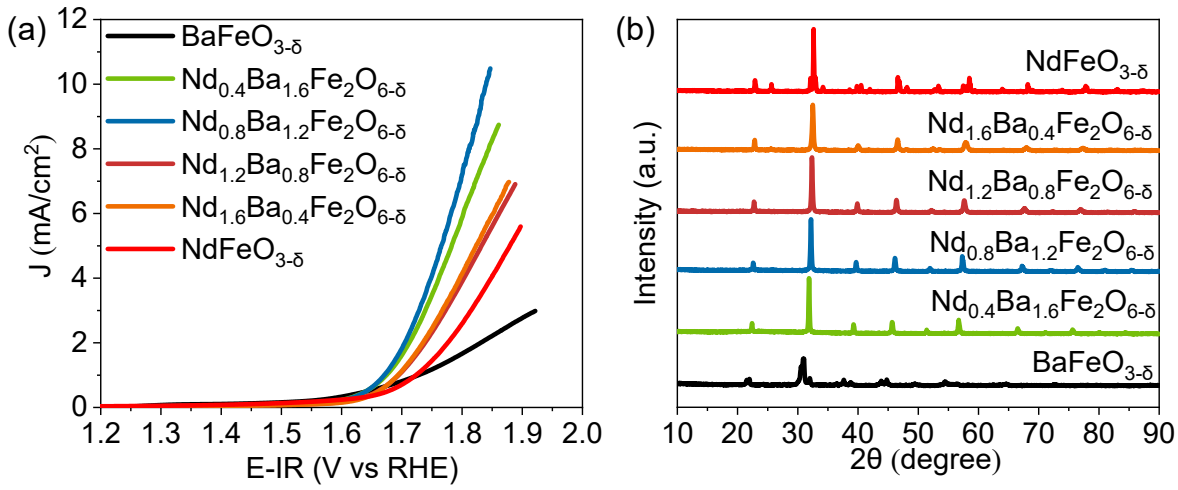

Figure S7 (a) LSV curves, (b) XRD pattern of $Nd_xBa_{2-x}Fe_2O_{6-\delta}$.

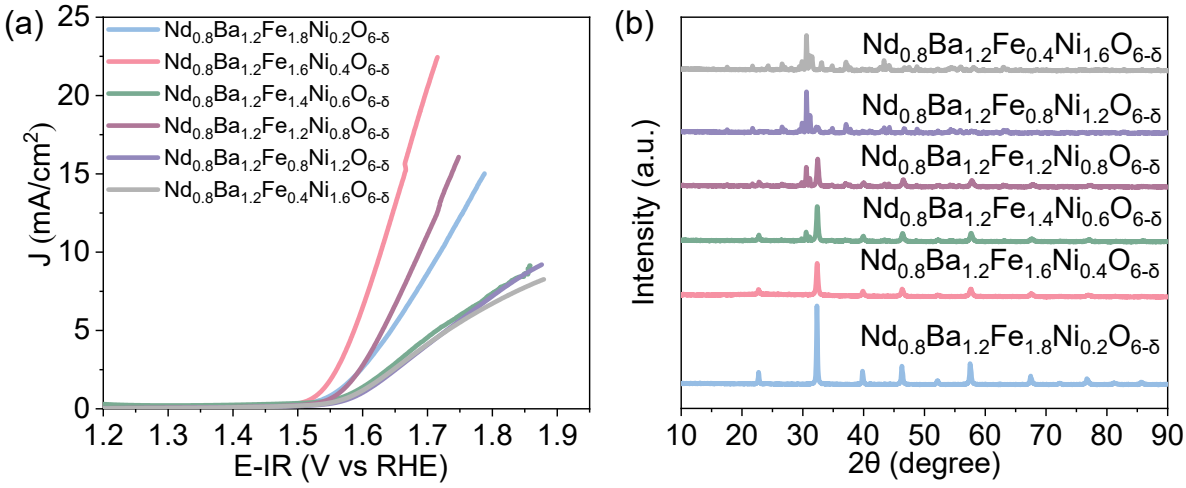

Figure S8 (a) LSV curves, (b) XRD pattern of $Nd_{0.8}Ba_{1.2}Fe_yNi_{2-y}O_{6-\delta}$.

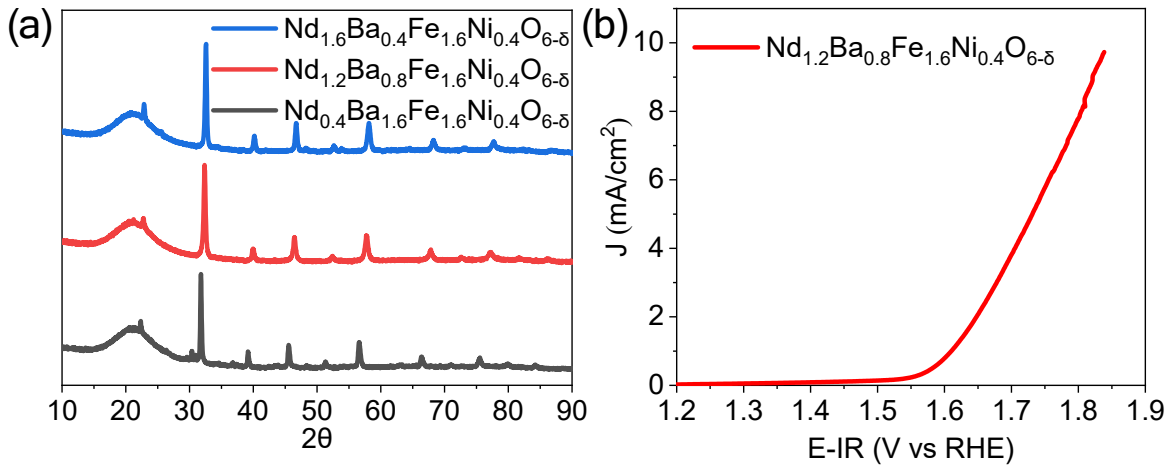

Figure S9 (a) XRD pattern of $Nd_xBa_{2-x}Fe_{1.6}Ni_{0.4}O_{6-\delta}$, (b) LSV curve of $Nd_{1.2}Ba_{0.8}Fe_{1.6}Ni_{0.4}O_{6-\delta}$.

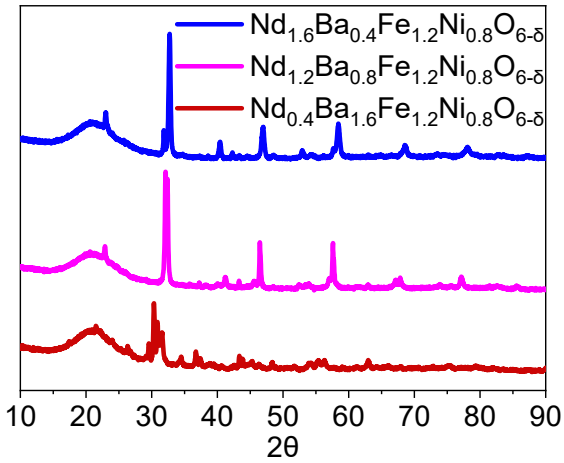

Figure S10 XRD pattern of $Nd_xBa_{2-x}Fe_{1.2}Ni_{0.8}O_{6-\delta}$.

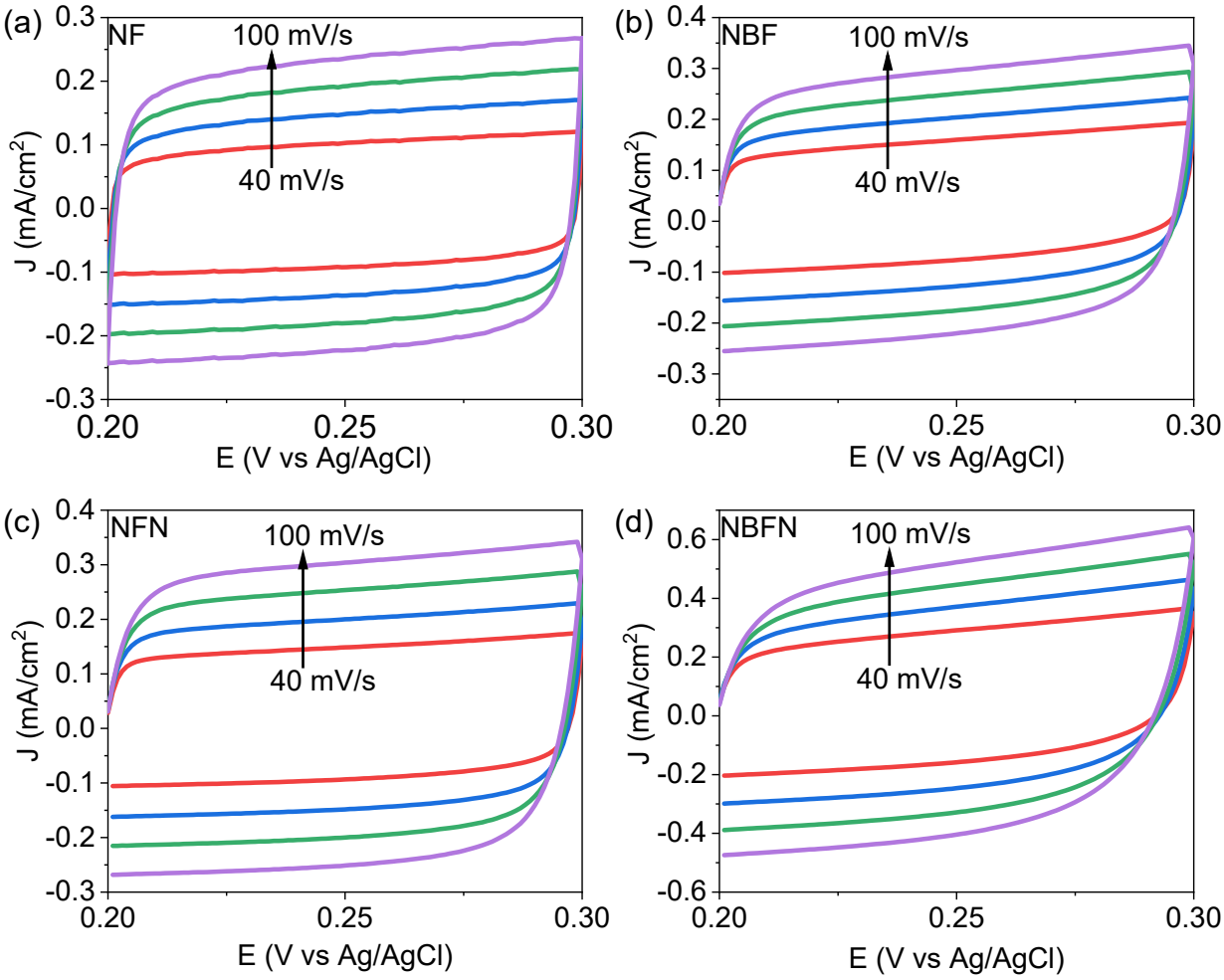

Figure S11 CVs of (a) NF, (b) NBF, (c) NFN and (d) NBFN at difference scan rates from 40 to 100 mA/s.

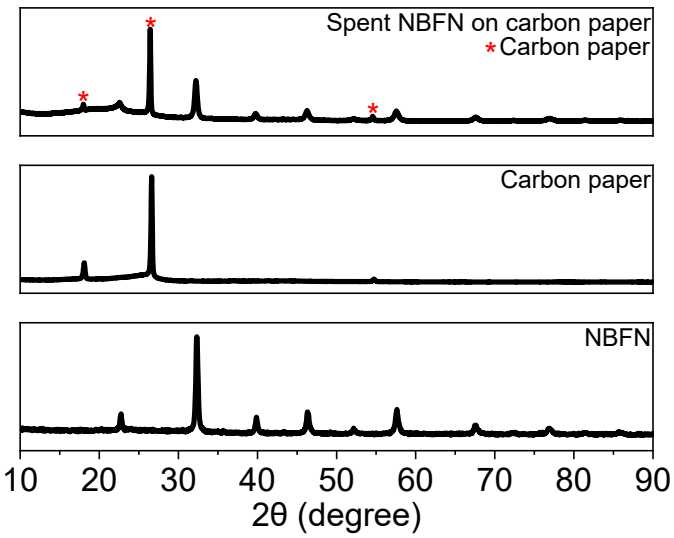

Figure S12 XRD pattern of fresh NBFN, carbon paper and NBFN loaded carbon paper after stability test.

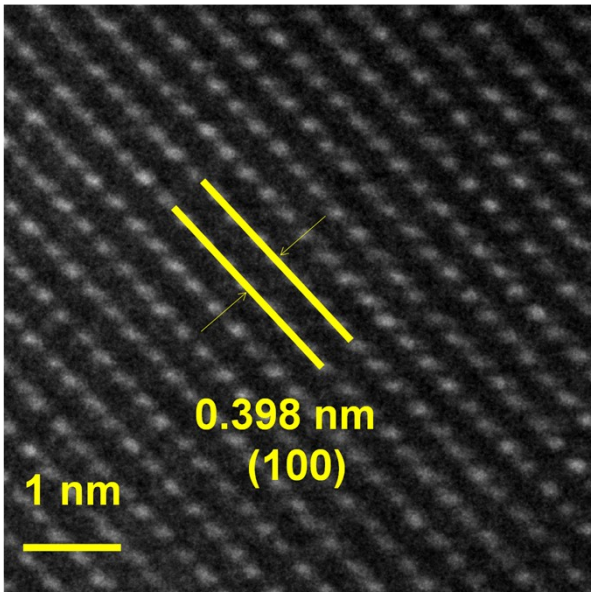

Figure S13 HR-TEM image of NBFN after stability.

Table S1 Composition study of NBFN through ICP.

Element	Atomic%
Nd	19.31%
Ba	29.22%
Fe	41.40%
Ni	10.07%

Table S2 The relative amounts of different surface oxygen species of NF, NBF, NFN and NBFN.

Composition	O^{2-} (%)	O^{2-}/O^{-} (%)	OH^{-}/O_2 (%)	H_2O (%)
NF	36.7396	13.9236	39.5124	9.8244
NBF	35.8741	29.4212	29.2694	5.4353
NFN	33.8339	21.7364	41.1509	3.2788
NBFN	26.3	23.3081	46.5457	3.8462

Table S3 The Fe valence state of NF, NBF, NFN and NBFN.

	Fe valence state
NF	3.1891
NBF	3.2143
NFN	3.0146
NBFN	3.0017

Table S4 Comparison of overpotential@10 mA/cm^2 with the literature.

Catalysts	Overpotential@10 mA/cm^2 (mV)	
$LaNiO_3$	449	[1]https://doi.org/10.1039/D1TA09306A
$La_{0.95}FeO_{3-\delta}$	410	[2]https://doi.org/10.1021/acs.chemmater.5b04457
BSCF	440	[3]https://doi.org/10.1002/cjoc.202100215
$SrNb_{0.1}Co_{0.7}Fe_{0.2}O_{3-\delta}$	420	[4]https://doi.org/10.1002/anie.201408998
$PrBaCo_2O_{5+\delta}$	520	[5]https://doi.org/10.1002/chem.201700507
$Sr_2Fe_{1.5}Mo_{0.5}O_{6-\delta}$	550	[6]https://doi.org/10.1016/j.seppur.2022.122316
$PrBa_{0.85}Ca_{0.15}FeMnO_{5+\delta}$	400	[7]https://doi.org/10.1021/acs.chemmater.7b01114
$LaCr_{0.5}Fe_{0.5}O_3$	390	[8]https://doi.org/10.1038/s41598-020-70283-9
RuO_2	390	[9]https://doi.org/10.1021/acscatal.7b02650
IrO_2	450	[10]https://doi.org/10.1039/C9TA01404G
This work	320	/

References:

[1] C. Liu, D. Ji, H. Shi, Z. Wu, H. Huang, Z. Kang, Z. Chen, An A-site management and oxygen-deficient regulation strategy with a perovskite oxide electrocatalyst for the oxygen evolution reaction, Journal of Materials Chemistry A, 10 (2022) 1336-1342.
[2] Y. Zhu, W. Zhou, J. Yu, Y. Chen, M. Liu, Z. Shao, Enhancing Electrocatalytic Activity of Perovskite Oxides by Tuning Cation Deficiency for Oxygen Reduction and Evolution Reactions, Chemistry of Materials, 28 (2016) 1691-1697.
[3] L. Tang, Y. Rao, L. Wei, H. Zheng, H. Liu, W. Zhang, K. Tang, A-site Cation Defects (Ba0.Sr.5)1–Co.Fe.O– Perovskites as Active Oxygen Evolution Reaction Catalyst in Alkaline Electrolyte†, Chinese Journal of Chemistry, 39 (2021) 2692-2698.
[4] Y. Zhu, W. Zhou, Z.-G. Chen, Y. Chen, C. Su, M.O. Tadé, Z. Shao, SrNb0.1Co0.7Fe0.2O3− Perovskite as a Next-Generation Electrocatalyst for Oxygen Evolution in Alkaline Solution, Angewandte Chemie International Edition, 54 (2015) 3897-3901.
[5] H. Sun, G. Chen, Y. Zhu, B. Liu, W. Zhou, Z. Shao, B-Site Cation Ordered Double Perovskites as Efficient and Stable Electrocatalysts for Oxygen Evolution Reaction, Chemistry – A European Journal, 23 (2017) 5722-5728.
[6] J. Zhou, T. Liu, J. Zhang, L. Zhao, W. He, Y. Wang, Rational design of ultrafine cobalt free electrospun nanofibers as efficient and durable binfunctional oxygen electrocatalysts for rechargeable zinc-air battery, Separation and Purification Technology, 304 (2023) 122316.
[7] B. Hua, Y.-F. Sun, M. Li, N. Yan, J. Chen, Y.-Q. Zhang, Y. Zeng, B. Shalchi Amirkhiz, J.-L. Luo, Stabilizing Double Perovskite for Effective Bifunctional Oxygen Electrocatalysis in Alkaline Conditions, Chemistry of Materials, 29 (2017) 6228-6237.
[8] X. Gao, Z. Sun, J. Ran, J. Li, J. Zhang, D. Gao, High efficiency electrocatalyst of LaCr0.5Fe0.5O3 nanoparticles on oxygen-evolution reaction, Scientific Reports, 10 (2020) 13395.
[9] J. Wang, Y. Gao, D. Chen, J. Liu, Z. Zhang, Z. Shao, F. Ciucci, Water Splitting with an Enhanced Bifunctional Double Perovskite, ACS Catalysis, 8 (2018) 364-371.
[10] H. Sun, X. Xu, Z. Hu, L.H. Tjeng, J. Zhao, Q. Zhang, H.-J. Lin, C.-T. Chen, T.-S. Chan, W. Zhou, Z. Shao, Boosting the oxygen evolution reaction activity of a perovskite through introducing multi-element synergy and building an ordered structure, Journal of Materials Chemistry A, 7 (2019) 9924-9932.